Chapter 7. Experimental Study on Classification

7.1 Characterization of Explosive Materials

7.1.1 Atomic effect number and density

Theoretically, most explosives fall within a relatively narrow window in Z_{eff} and in density, and can be distinguished from other organic and inorganic materials (see Figure 7.1-1). For a compound material, the effective atomic number Z_{eff} is the characteristic value of a hypothetical substance having an equivalent x-ray attenuation effect as the compound. We assume that a material is a uniform compound consisting of M elements, having an atomic number Z_i and contributing mass m_i. Z_{eff} can be estimated with following formula [JOH83] [EIL96],

$$Z_{eff} = \left(\sum_{i=1}^{M} a_i \cdot Z_i^{3.5} \Big/ \sum_{i=1}^{M} a_i \right)^{1/3.5} \tag{7.1}$$

where $a_i = m_i \cdot Z_i / A_i$, and A_i is the atomic weight for element i. From (7.1), it is known that to estimate Z_{eff} of a compound, we need to estimate how many elements are in the compound, what they are, and to measure or estimate the contributing mass of each element. It is almost impossible to get this information by using dual-energy transmission and scatter x-ray

imaging techniques so far. Nor can the density of a compound be measured directly with single view dual-energy system.

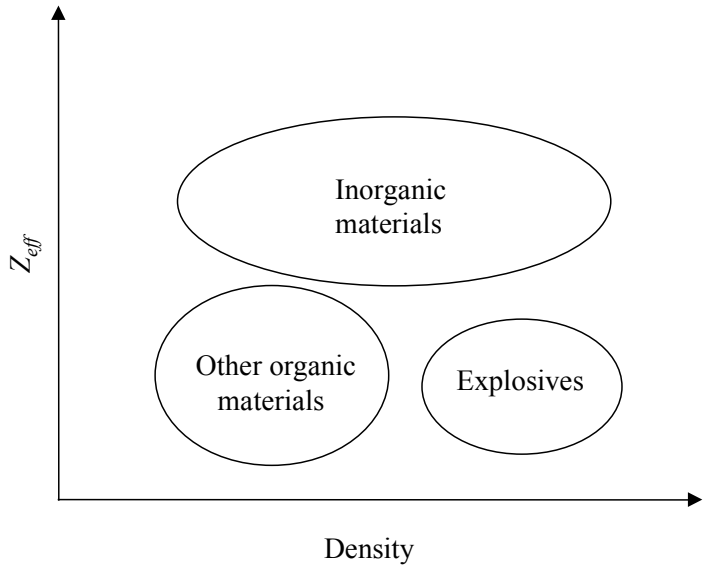

Figure 7.1-1 Characterization of common materials found in luggage.

7.1.2 Classification feature space in the prototype scanning system

As stated in Chapter 1, the overall goal of this research is to develop an x-ray scanning system that uses dual-energy transmission and scattering to detect explosives. To realize this goal, six types of images are available in the prototype scanning system. Right now, four of them are processed to classify material types. They are,

- Transmission of high energy: T_H
- Transmission of low energy: T_L

- Back scatter of low energy: B_L
- Forward scatter of low energy: F_L

By combining these sensors together, a feature vector in 2-dimensional space (R, L) is formed with Equations 7.2 and 7.3. Any object scanned in the luggage bags will be mapped onto this 2-dimensional plane.

$$R = \frac{\psi_i}{\psi_j} \tag{7.2}$$

$$L = \frac{\log\left(a_0 F_L + a_1 F_L^2 + b_0 B_L + b_1 B_L^2\right)}{\log(T_L)} \tag{7.3}$$

In these equations, ψ_i and ψ_j are the area attenuation coefficients, estimated by *Algorithm* 5.1, at low and high x-ray energies respectively; a_0, a_1, b_0, and b_1 are coefficients found in Equation 6.12 or Equation 6.15. Actually, R is close to Z_{eff}, and is fairly good at distinguishing organic materials from inorganic materials. L is related to density, and is very effective for separating thin materials from thick materials.

Figure 7.1-2 gives an example scanned from real luggage bags. In the figure, six explosive simulants provided by FAA are represented as "+". They are simulants for high-density ammonia nitrate, low density ammonia nitrate, smokeless powder, black powder, semtex, and dynamite. The explosive simulants will be described further in Section 7.3. Three step wedges, represented as "o", are shown in three different boxes. Other materials, such as clothes, shoes, books, plastics, woods, toiletry formulations, chocolates, and so on, are also represented as "o". We see that (R, L) is a pretty good feature space. Based on (R, L), statistical decision rules have been developed to distinguish explosives from other materials.

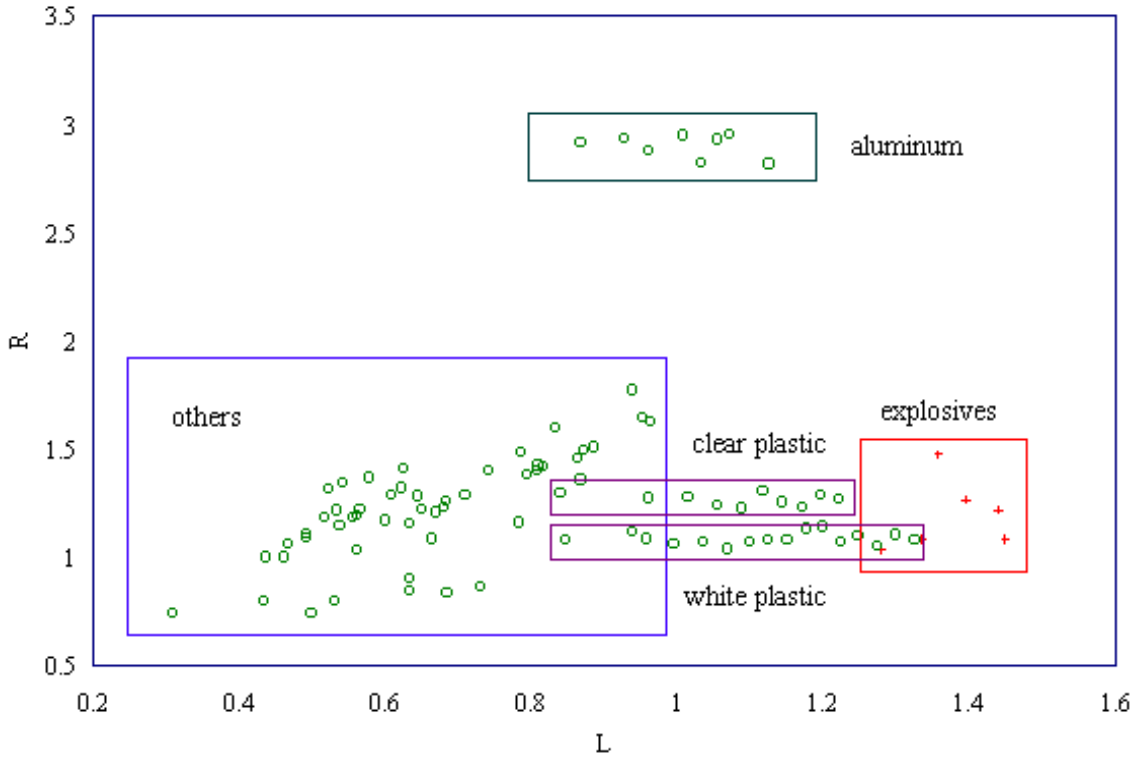

Figure 7.1-2 Measurements on real luggage materials, step wedges and explosive simulants: "+" represents explosive simulants, "o" represents the other materials.

7.2 Test Objects

7.2.1 Description of test objects

To verify the capability and to study the limitations of material characterization method, experiments were performed using particular test objects and actual passenger luggage bags, with and without explosive simulants. Twenty unclaimed luggage bags were purchased from a major airline. Also, we obtained some explosive simulants in two orders from FAA; they are plastic simulants, and explosive simulants.

By inserting different objects into these luggage bags, hundreds of experimental scenarios were created. The objects that were inserted into bags include: explosive simulants, white and clear plastic step wedges, an aluminum step wedge, a walkman player, shampoo bottles, bottles of honey, sugar, hair dryers, pillows, clothes, towels, books, a steel step wedge, etc. A typical bag is shown on Figure 7.2-1, where (a) gives the outward appearance, and (b) shows some contents inside.

Our research efforts focused on detecting explosives in luggage. But using real explosives as the testing objects poses serious safety concerns at a university. The SDA lab does not have the necessary means to obtain, transport, and store these hazardous materials. However, to perform meaningful experiments some types of illicit materials have to be used. Explosive simulants are believed to be resonable substitutes for the real explosives. Explosive simulants are inert materials that exhibit accurately controlled physical properties. They specifically and reliably duplicate selected characteristics, such as density and Z_{eff}, of real explosive materials, and those characteristics are recognized by using explosive detection technologies such as x-ray detection technologies [EIL96] [SPA96].

Rigid plastics were also used in this work. They have limited usefulness in accurately simulating explosive devices, training operators, and testing automated detection systems that use x-rays. The plastic simulants in our study are shown in Figure 7.2-2. They have a similar Z_{eff} to the actual explosives, but not the same density.

Figure 7.2-3 shows a picture of six explosive simulants. They are all members of a new class of explosive simulants. These simulants are mixtures of two or more components. The inert properties of each component have been verified by analyses, and none of these components is regulated by the government. They closely match both the Z_{eff} and density of real explosives. Also since they are all powders, this makes them like real explosives as well. All these simulants have demonstrated stability of more than six months, as long as they are appropriately wrapped and stored. Description of both explosive and plastic simulants is listed in Table 7.2-1.

Table 7.2-1 List of standard simulants used in the experimental study

Simulant name	Description
RXN-08-AJ	Simulant for smokeless powder
RXN-11-GE-AB	Simulant for high-density ammonia nitrate
RXN-07-AE	Simulant for black powder
RXN-04-AF	Simulant for semtex
RXN-06-AF	Simulant for dynamite
RXN-10-AF	Simulant for low-density ammonia nitrate
Plastic #1	Solid square plastic object
Plastic #2	Solid square plastic object
Plastic #3	Solid square plastic object
Plastic #4	Bundle of three solid cylinder plastic objects

(a)

(b)

Figure 7.2-1 A typical luggage bag used in these experiments. (a) Outward appearance. (b) Contents of the bag.

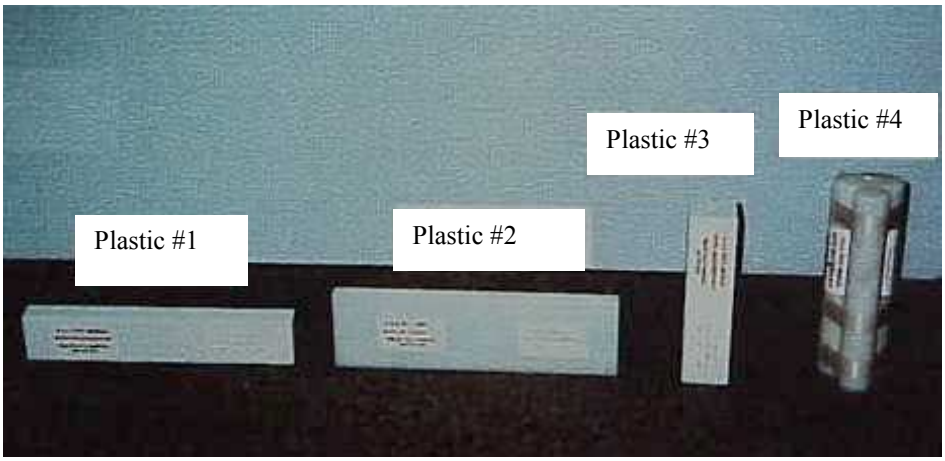

Figure 7.2-2 Plastic simulants used in this research.

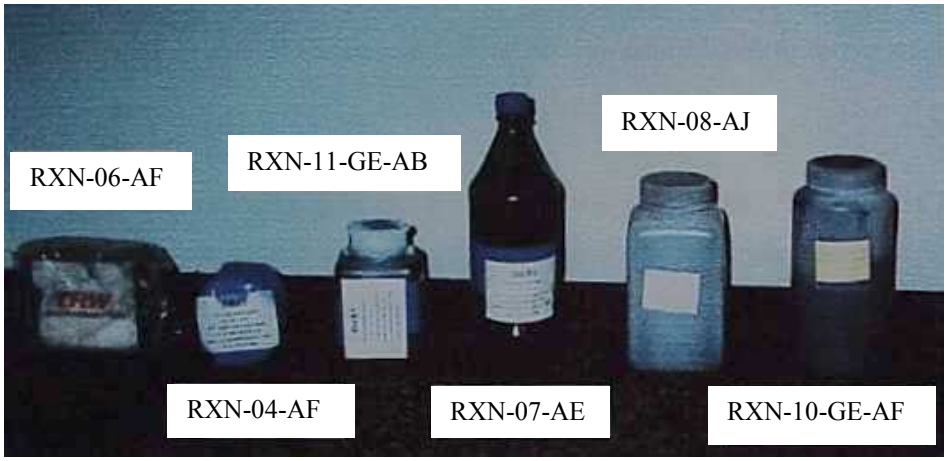

Figure 7.2-3 Explosive simulants used in this research.

7.2.2 Image examples collected using the prototype scanner

For each scenario, images were collected using the prototype x-ray scanning system. As stated in Section 7.1.2, these images include a high-energy transmission image, a low-energy transmission image, a low-energy backward scattering image and a low-energy forward scattering image.

Figure 7.2-4 shows the images scanned for six explosive simulants. From left to right, they represent smokeless powder, high-density ammonia nitrate, black powder, semtex, dynamite, and low-density ammonia nitrate. From the figure, we can observe that explosive simulants exhibit only a small difference between low and high transmissions, and have a high scattering. This characterization is what we have seen in the previous section, where they fall in a block having higher value of L in (R, L) space.

Figure 7.2-5 gives the images scanned for four plastic simulants. They are packaged in a typical test bag from FAA. They have similar characteristics as the explosive simulants.

The scattering images for three step wedges are given in Figures 7.2-6 to 7.2-8. Their transmission images have been shown in Section 5.1-4 through Figures 5.1-7 to 5.1-9. Step wedges are very useful to our experimental study in this dissertation based on the following considerations: 1) aluminum step wedges stand for a typical object of inorganic material, while white and clear plastic step wedges are typical objects of organic material; 2) by considering step wedges, we can verify the thickness effects on both transmission and scatter imaging; 3) by using step wedges, it is very convenient to evaluate new methods for improving object classification (such as with or without copper filter, the numerical method, and so on). Several typical imaging examples of luggage bags are given in Figures 7.2-9 to 7.2-12.

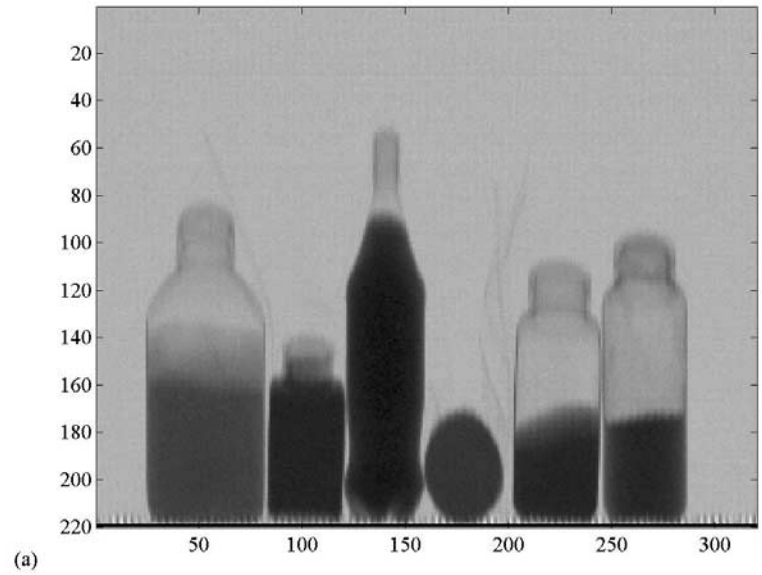

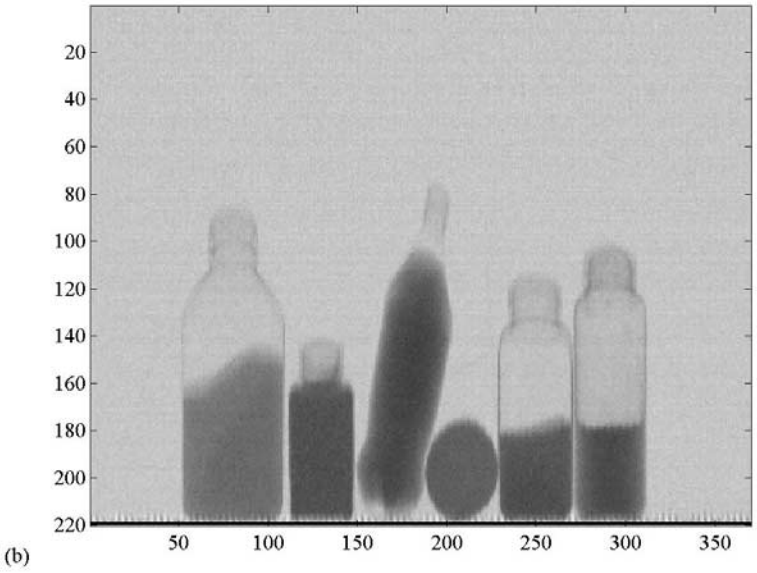

Figure 7.2-4 Images scanned for six explosive simulants: (a) low-energy transmission, (b) high-energy transmission.

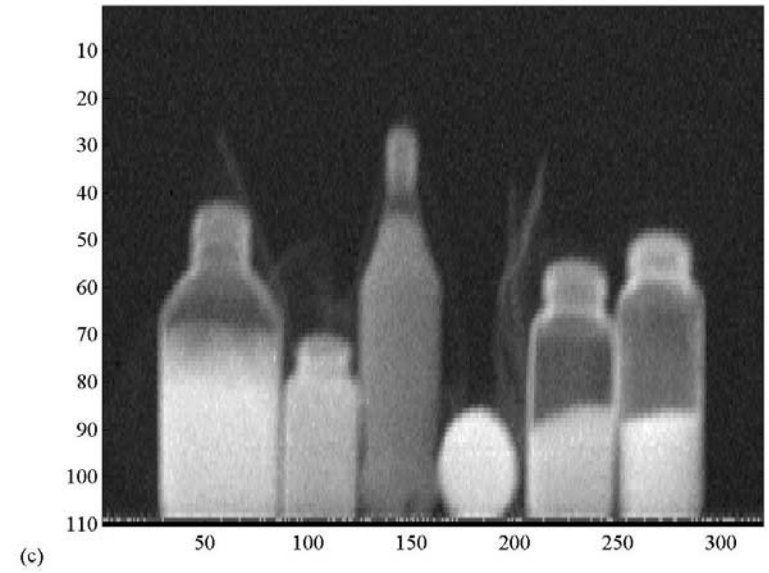

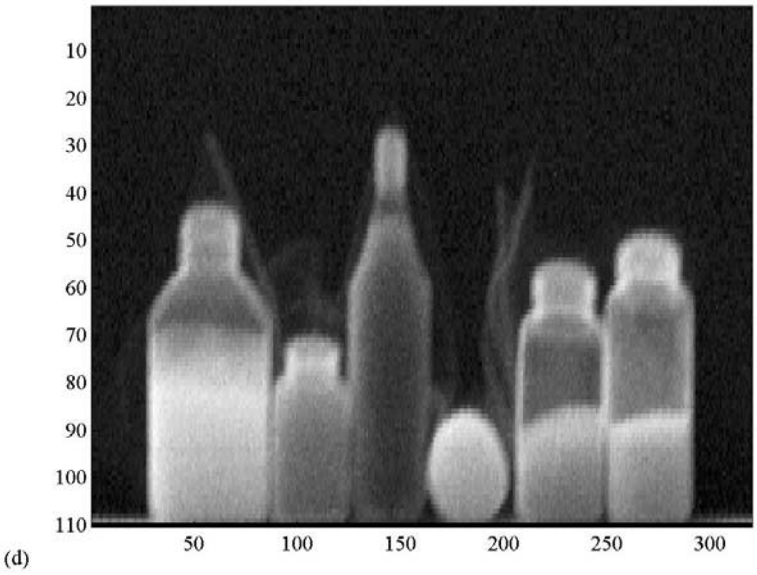

Figure 7.2-4, continued. (c) Low-energy backward scattering, and (d) low-energy forward scattering.

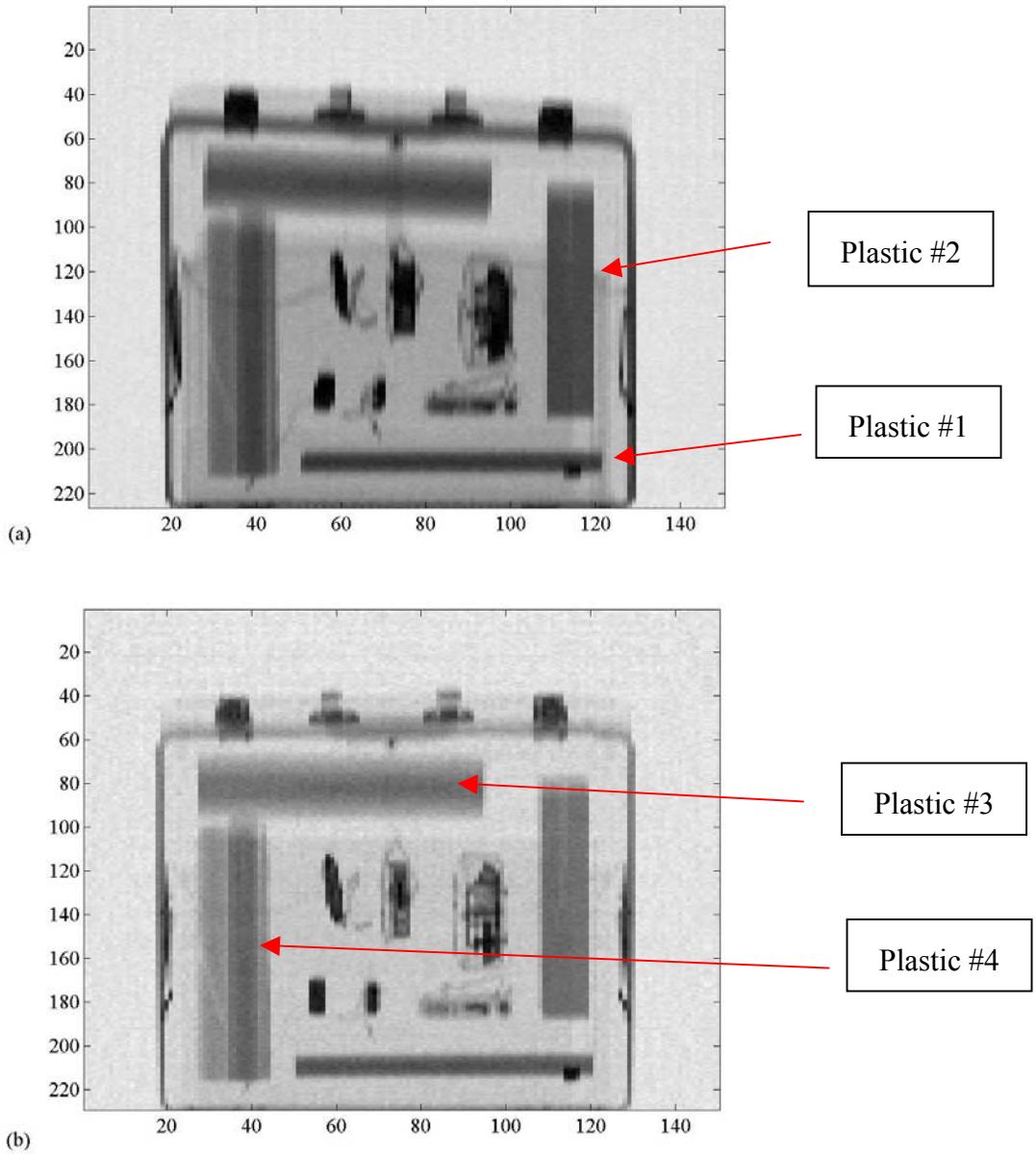

Figure 7.2-5 Images scanned for plastic simulants: (a) low-energy transmission, (b) high-energy transmission.

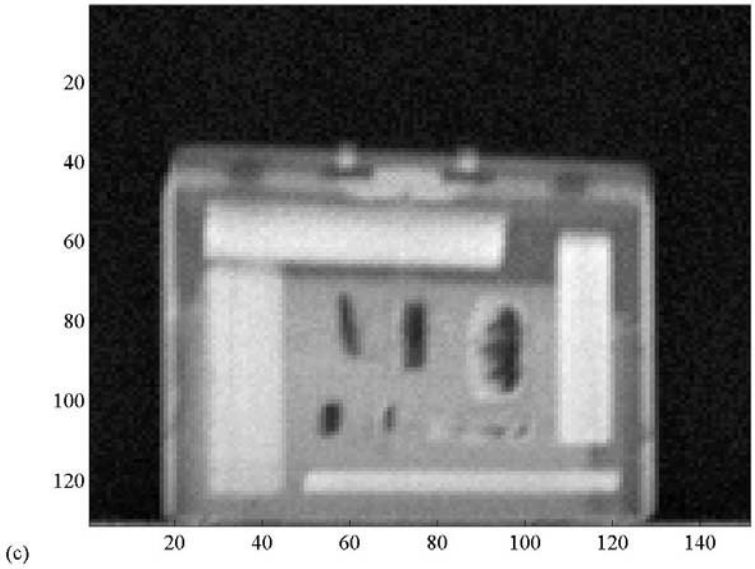

(c)

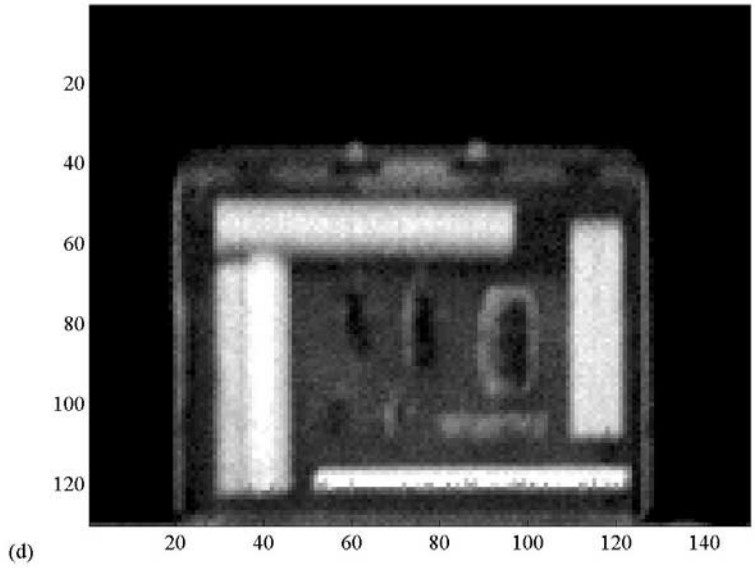

(d)

Figure 7.2-5, continued. (c) Low-energy backward scattering, and (d) low-energy forward scattering.

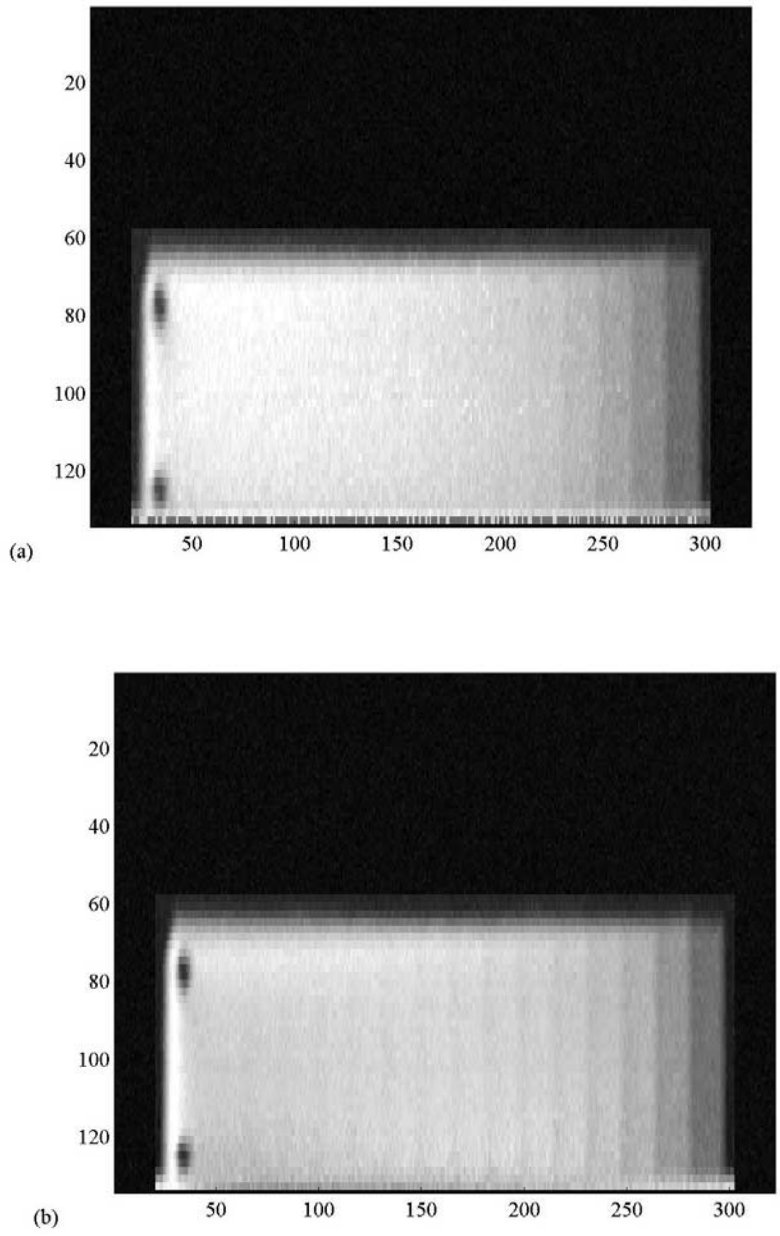

Figure 7.2-6 Images scanned for white plastic step wedge: (a) low-energy backward scattering, and (b) low-energy forward scattering.

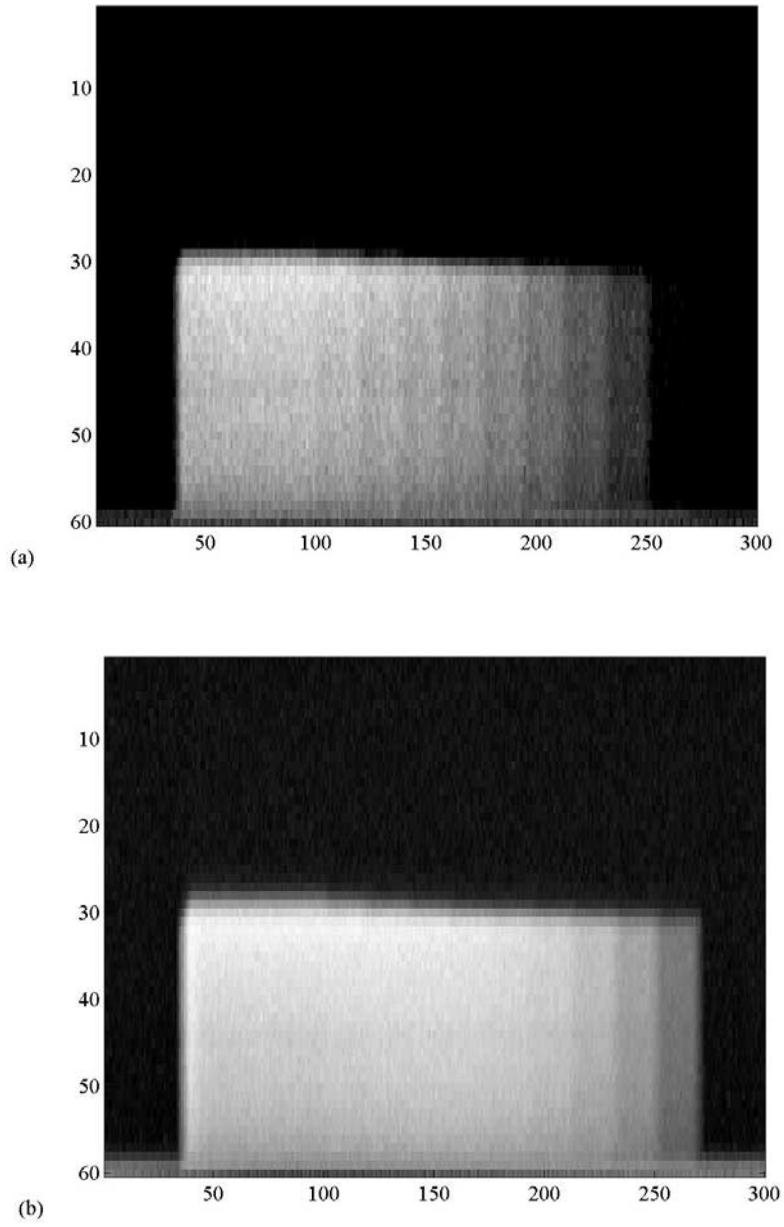

Figure 7.2-7 Images scanned for clear plastic step wedge: (a) low-energy backward scattering, and (d) low-energy forward scattering.

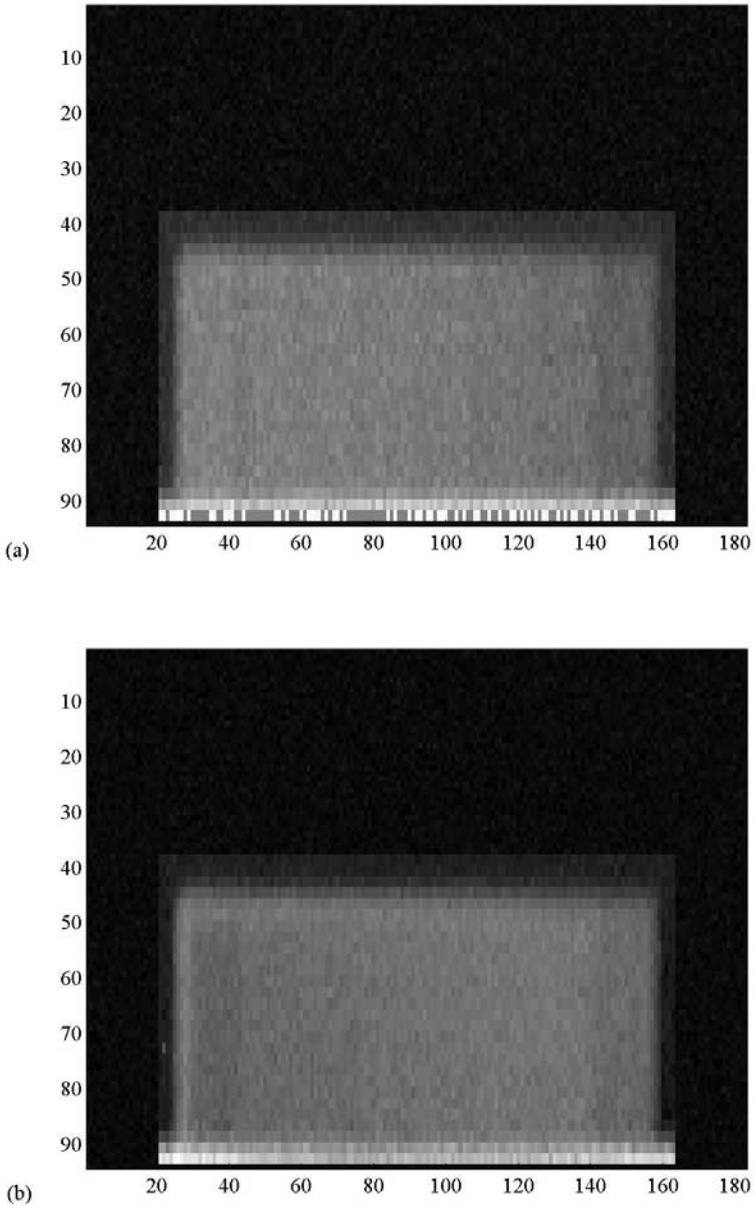

Figure 7.2-8 Images scanned for aluminum step wedge: (a) low-energy backward scattering, and (d) low-energy forward scattering.

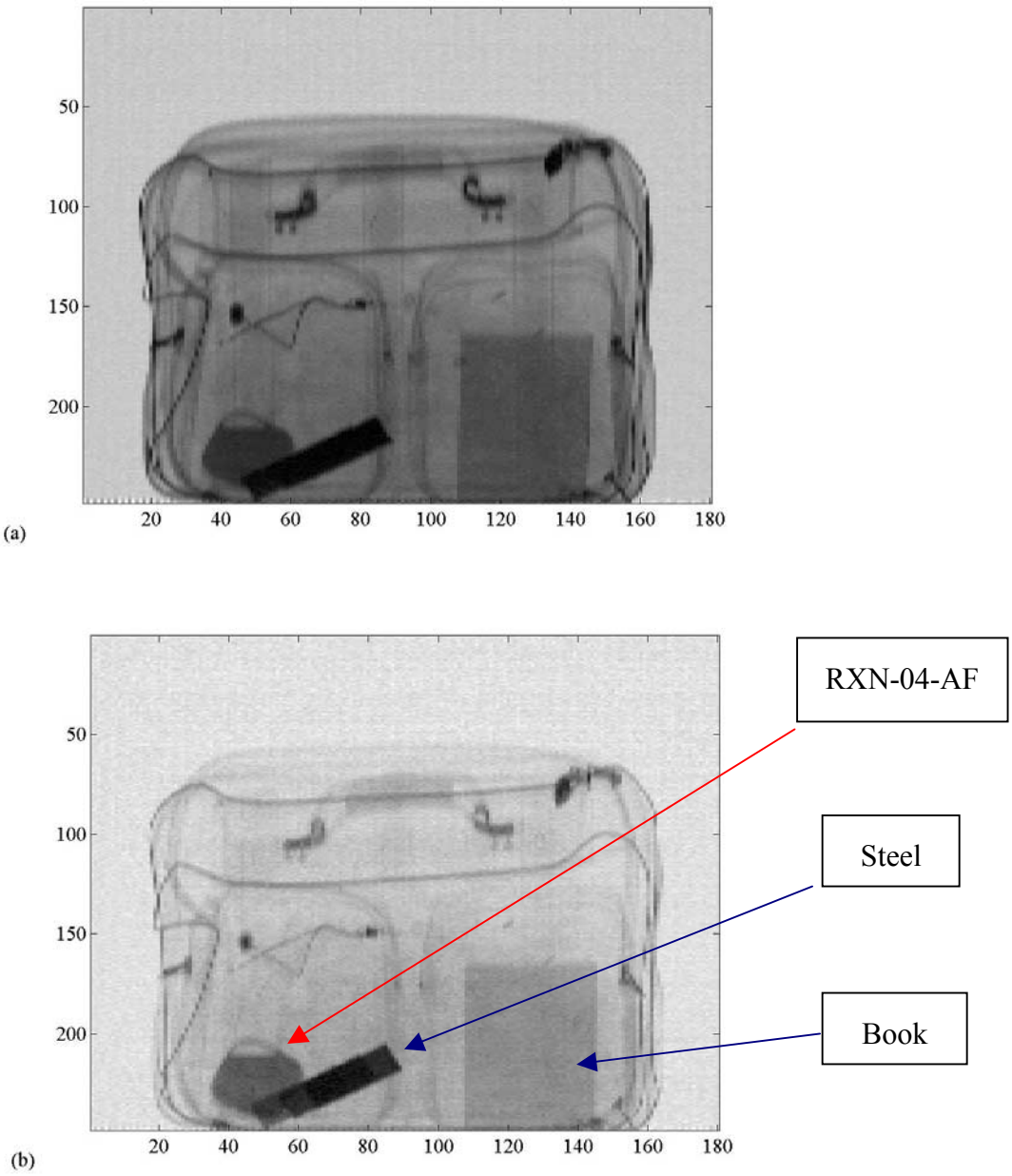

Figure 7.2-9 Images scanned for a common luggage bag with one explosive simulant: (a) low-energy transmission, and (b) high-energy transmission.

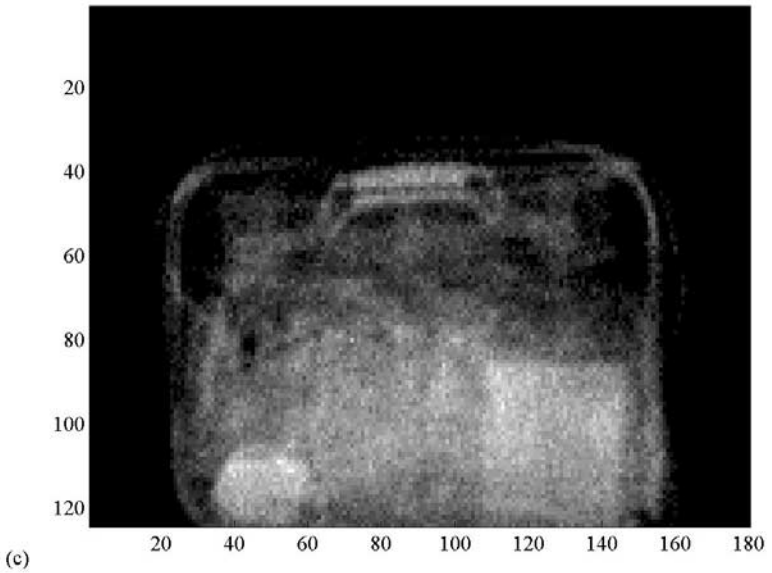

(c)

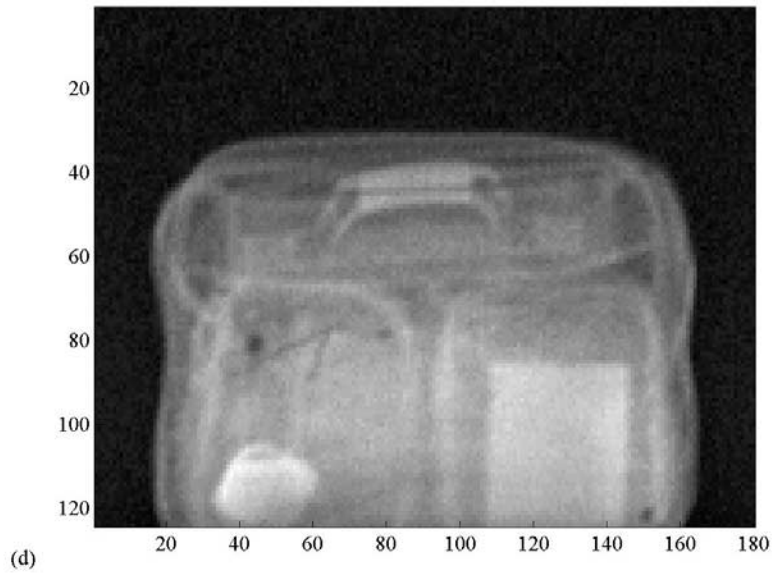

(d)

Figure 7.2-9, continued. (c) Low-energy backward scattering, and (d) low-energy forward scattering.

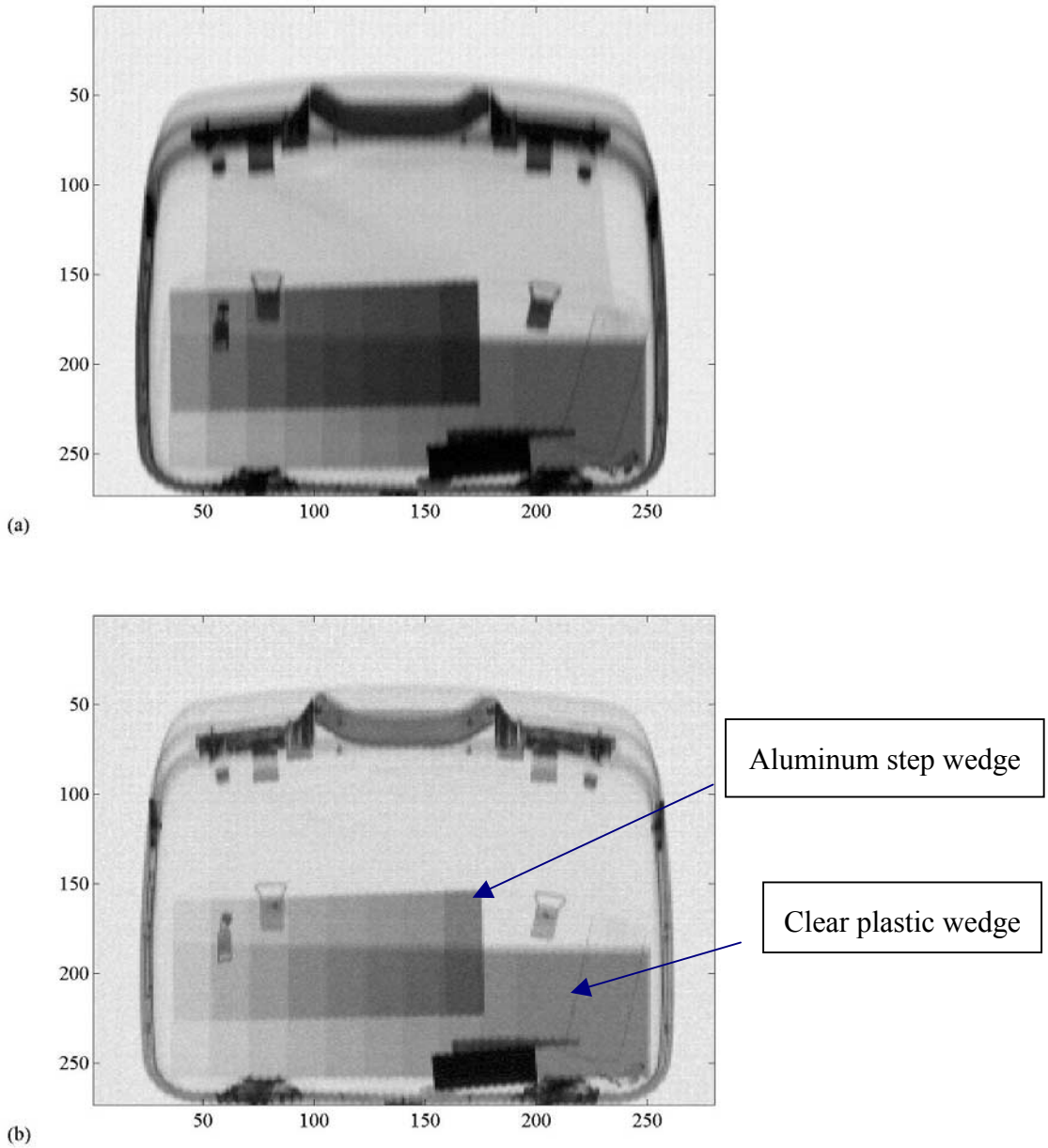

Figure 7.2-10 Images scanned for a common luggage bag inserted with two step wedges: (a) low-energy transmission, and (b) high-energy transmission.

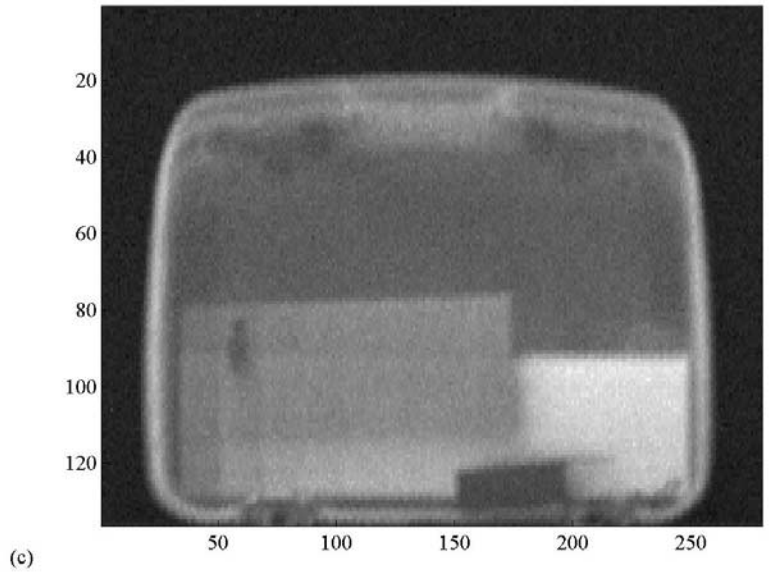

(c)

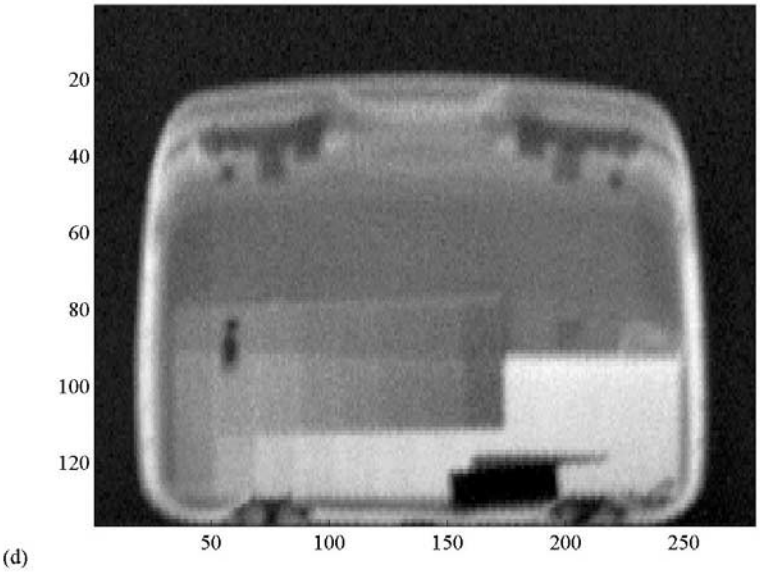

(d)

Figure 7.2-10, continued. (c) Low-energy backward scattering, and (d) low-energy forward scattering.

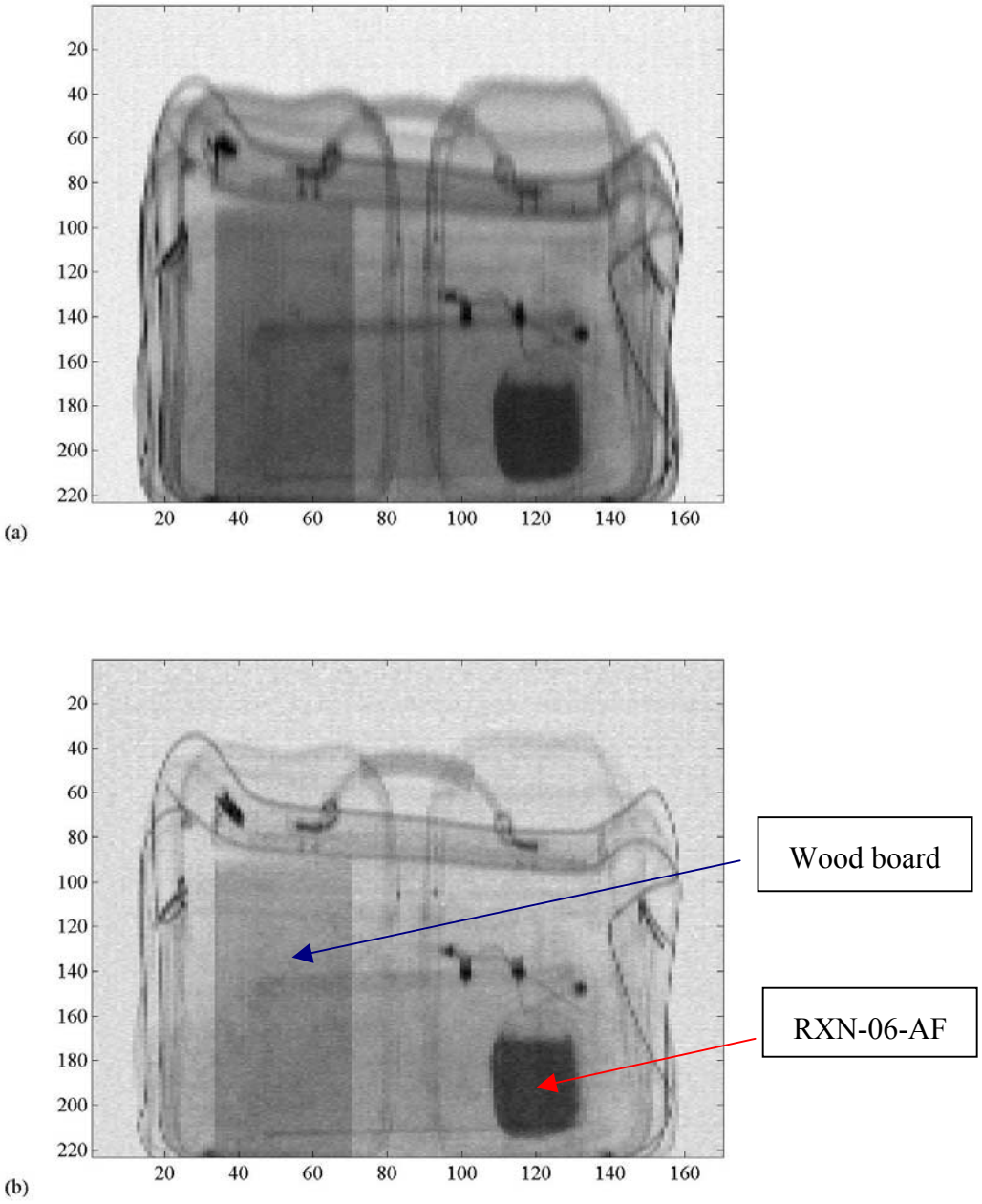

Figure 7.2-11 Images scanned for a common luggage bag with one explosive simulant: (a) low-energy transmission, and (b) high-energy transmission.

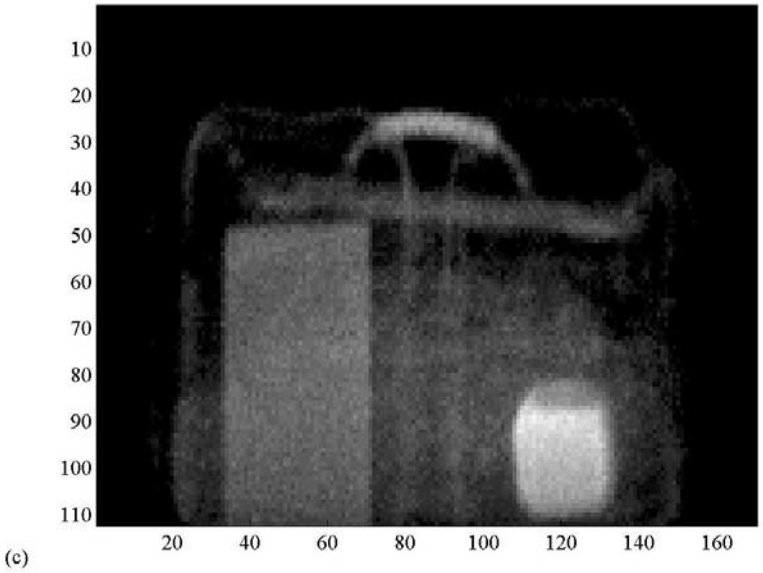

(c)

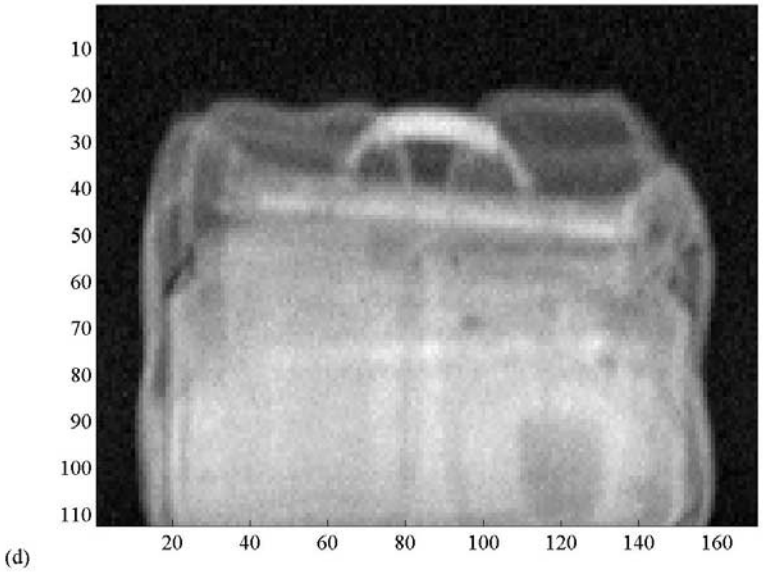

(d)

Figure 7.2-11, continued. (c) low-energy backward scattering, and (d) low-energy forward scattering.

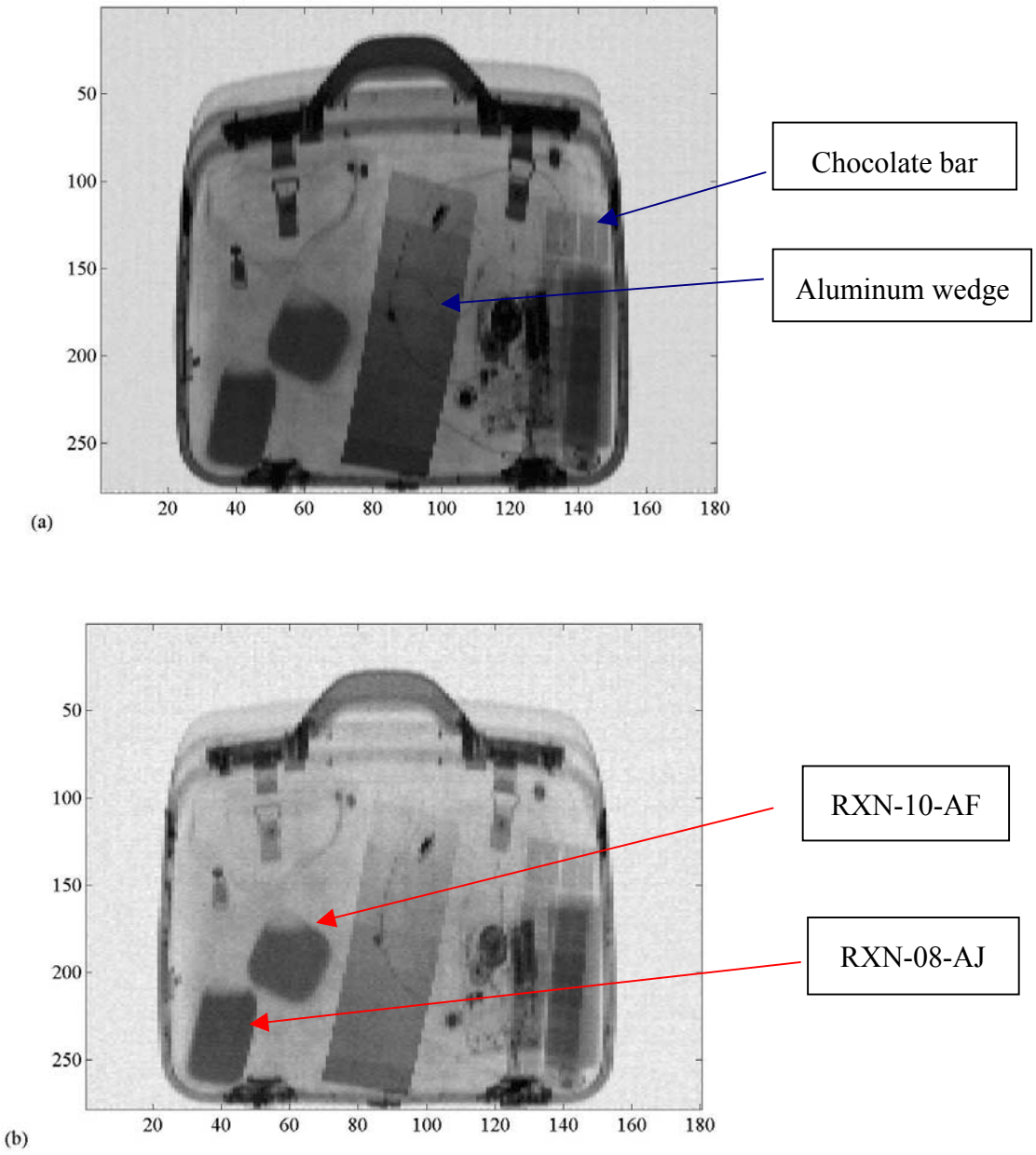

Figure 7.2-12 Images scanned for a common luggage bag with three explosive simulants: (a) low-energy transmission, and (b) high-energy transmission.

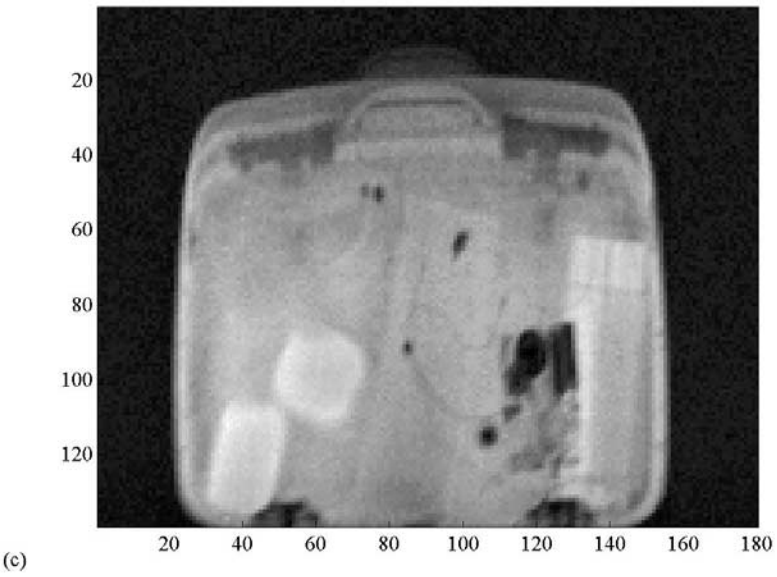

(c)

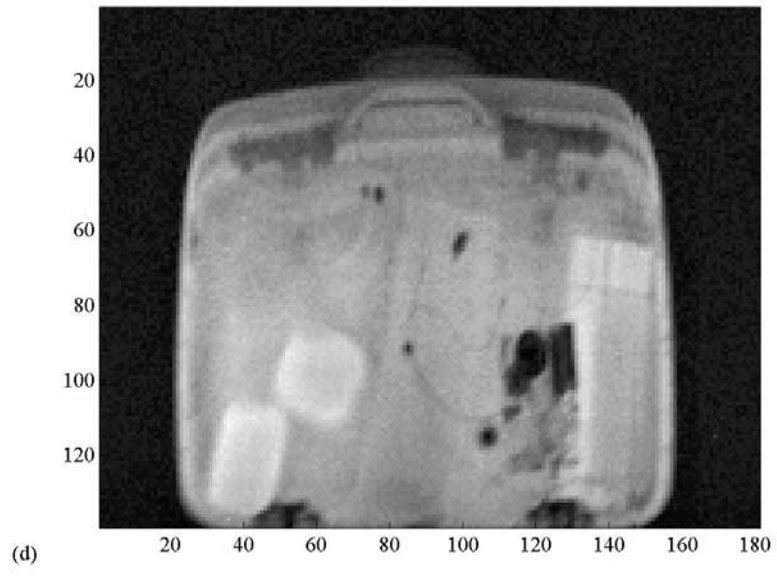

(d)

Figure 7.2-12, continued. (c) Low-energy backward scattering, and (d) low-energy forward scattering.

7.3 Experimental Study on Classification

7.3.1 Bayes decision theory

Bayes decision theory serves as a fundamental statistical approach to the problem of pattern recognition. This approach is based on the assumption that the decision problem is posed in probabilistic terms, and that all of the relevant probabilities are known [DUD73] [SCH96] [SCH92]. We assume this is the case in our analysis on material characterization. The feature vector x, which will be used in analysis, combines dual-energy and scattering measurements, (R, L).

Let $p(x \mid C_j)$ be the probability density function for x given that the state of nature is C_j, where $C_j \in \Omega = \{C_1, C_2, \cdots, C_s\}$, and s is the number of states of nature. In this dissertation, C_j represents the material type j characterized by R and L. Then the difference between $p(x \mid C_k)$ and $p(x \mid C_i)$ describes how likely that material k may be distinguished from material i in $R-L$ feature space. Suppose that we know both the a priori probability $P(C_j)$ and the conditional density $p(x \mid C_j)$. Suppose further that we measure $x = (R, L)$, the a posteriori probability, $P(C_j \mid x)$, then can be computed from a priori probability and conditional density by Bayes rule [DUD73]:

$$P(C_j \mid x) = \frac{p(x \mid C_j) P(C_j)}{p(x)} \tag{7.4}$$

where

$$p(x) = \sum_{j=1}^{s} p(x \mid C_j) P(C_j) \tag{7.5}$$

Suppose that we observe a particular measurement x and that we contemplate taking an action α_i, where $\alpha_i \in A = \{\alpha_1, \alpha_2, \cdots, \alpha_a\}$, and a is the number of possible actions. If the true state of nature is C_j, we will incur the loss $\lambda(\alpha_i \mid C_j)$. Since $p(C_j \mid x)$ is the probability that the true state of nature is C_j, the expected loss associated with taking action α_i is

$$\Theta(\alpha_i \mid x) = \sum_{j=1}^{s} \lambda(\alpha_i \mid C_j) P(C_j \mid x) \tag{7.6}$$

In decision theoretic terminology, an expected loss is called a risk, and $\Theta(\alpha_i \mid x)$ is known as the conditional risk. Whenever we encounter a particular observation x, we can minimize our expected loss by selecting the action that minimizes the conditional risk. This justifies the following statement of the Bayes decision rule: To minimize the overall risk, compute the conditional risk $\Theta(\alpha_i \mid x)$ with (7.6) for $i = 1, 2, \cdots, a$ and select the action α_i for which $\Theta(\alpha_i \mid x)$ is minimum. Two possible "actions", identification as explosives or other materials, could be taken in the context of luggage scanning.

7.3.2 Minimum-error-rate classification

In classification problems, each state of nature is usually associated with a certain class. If action α_i is taken and the true state of nature is C_j, then the decision is correct if $i = j$, and in error if $i \neq j$. If errors are to be avoided, it is natural to seek a decision rule that minimizes the average probability of error, i.e., the error rate.

A loss function of particular interest for this case is the so-called symmetrical or zero-one loss function [DUD73],

$$\lambda(\alpha_i \mid C_j) = \begin{cases} 0 & \text{for } i = j \\ 1 & \text{for } i \neq j \end{cases} \tag{7.7}$$

This loss function assigns no loss to a correct decision, and a unit loss for any error. From (7.4), the conditional risk is thus equal to,

$$\Theta(\alpha_i \mid x) = \sum_{j=1}^{s} \lambda(\alpha_i \mid C_j) P(C_j \mid x) = 1 - P(C_i \mid x) \tag{7.8}$$

Since $P(C_i \mid x)$ is the conditional probability that action α_i is correct, the overall risk is precisely the average probability of error. Remember that Bayes rule minimizes risks by selecting the action that minimizes the conditional risk. Thus to minimize the average probability of error, we should select C_i that maximizes the a posteriori probability $P(C_i \mid x)$. In other words, for minimum error rate, decide C_i if $P(C_i \mid x) > P(C_j \mid x)$ for all $j \neq i$.

7.3.3 Classifiers, discriminant functions and decision boundaries

There are many different ways to represent pattern classifiers. One way is in terms of a set of discriminant functions $g_i(x)$, $i = 1, \cdots, s$, [DUD73]. The classifier is said to assign a feature vector x to class C_i if

$$g_i(x) > g_j(x), \qquad \text{for all } j \neq i \tag{7.9}$$

The classifier, therefore, is viewed as a machine that computes *s* discriminant functions and selects the category corresponding to the largest discriminant. This representation of a classifier is illustrated in Figure 7.3-1.

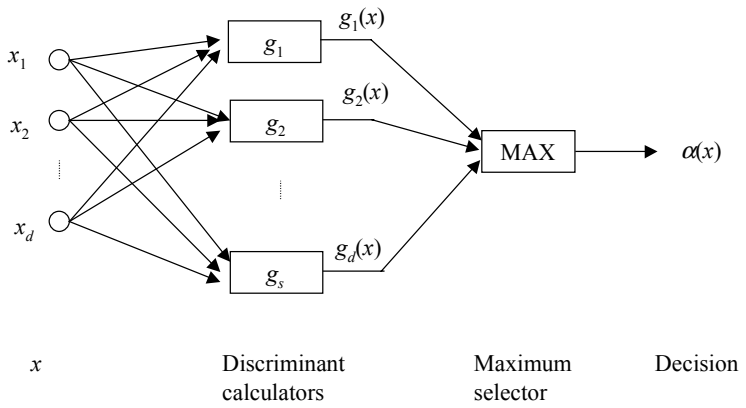

Figure 7.3-1 A pattern classifier [DUD73].

A Bayes classifier can be easily represented in this way. Generally, we can let $g_i(x) = -\Theta(\alpha_i \mid x)$, since the maximum discriminant function will then correspond to the minimum conditional risk. For the minimum error rate case, we can simplify the expression further by taking $g_i(x) = P(C_i \mid x)$, so that the maximum discriminant function corresponds to the maximum a posteriori probability.

It should be pointed out that the choice of the discriminant functions is not unique. We can always multiply the discriminant functions by a positive constant or bias them by an additive constant without influencing the decision. For a more general case, if we replace every $g_i(x)$ by $f(g_i(x))$, the resulting classification is unchanged as long as $f()$ is a monotonically

increasing function. This observation can lead to significant analytical and computational simplifications.

Even though the discriminant functions can be written in a variety of forms as stated above, the decision rules are equivalent. The effect of any decision rule is to divide the feature space into s regions, which can be represented as, $\Re_1$, $\Re_2$, …, $\Re_s$. If $g_i(x) > g_j(x)$ for all $j \neq i$, then we say that x is in $\Re_i$, and decision rule calls us to assign x to C_i. The regions are separated by decision boundaries, surfaces in the feature space where ties occur among the largest discriminant functions. If $\Re_i$ and $\Re_j$ are contiguous, the equation for the decision boundary is

$$g_i(x) = g_j(x) \tag{7.10}$$

For points on the decision boundary the classification is not uniquely defined. Because the conditional risk associated with either decision is the same for the Bayes classifier, it does not matter how ties are broken.

7.3.4 Classification rules in the prototype x-ray imaging system

The two-category classification problem is merely a particular case of above discussion, where $\Omega = \{C_1, C_2\}$ and $A = \{\alpha_1, \alpha_2\}$. Let C_2 be explosives and C_1 stand for other materials, suppose we want to detect C_2 from C_1; then under the assumptions stated earlier $\Theta(\alpha_1 \mid x \in C_2)$ is the probability of missed detection, and $\Theta(\alpha_2 \mid x \in C_1)$ is the false alarm rate.

In this dissertation, a statistically determined decision boundary is used to distinguish explosives from other materials. From theoretical analysis and experimental measurements, it

is known that: 1) explosives fall in a region of the (R, L) space, not a point; 2) we have only a limited set of testing materials, both explosive simulants and innocent materials; 3) decision surfaces of separating explosives from other materials are not convex. So the proposed classification procedure is as follows:

- Threshold on transmission imaging. A threshold is selected for removing the objects exhibiting high attenuation. This may be caused either by high *Z* materials or by very thick low *Z* materials. In this case, x-rays are not strong enough to penetrate the material, resulting in a bigger error.
- Discriminant functions. There are only two discriminant functions for our case. They are $g_1(x) = p(x \mid C_1)P(C_1)$ and $g_2(x) = p(x \mid C_2)P(C_2)$ respectively. The a priori probability $P(C_j)$ can be selected as follows: 1) for the system test at laboratories, we can set $P(C_1) = P(C_2) = 0.5$, which means that explosives and other materials are equally likely to appear in luggage bags; 2) for the luggage scanning at airports, we may select $P(C_1) > P(C_2)$, depending on the risks of missed detection and false alarm. The discriminant function $g_i(x)$, therefore, is only determined by the probability density function $p(x \mid C_i)$.
- Decision boundary. Two methods have been used to design decision boundaries in this research. 1) Under the assumption of normal distributions, it is possible to estimate the parameters of $p(x \mid C_j)$ by using the measurement data. The procedure is as follows: (a) compute the mean values μ_j and covariance matrix Ω_j for both classes: explosives and other materials; (b) obtain the normal density functions $p(x|C_j)$; (c) draw the decision boundary, which satisfies $p(x|C_1) = p(x|C_2)$. In Section 7.3-5, a decision boundary based on the approach above will be shown as an example. 2) A piecewise linear boundary can also be used to distinguish explosives from other materials. The reason to use piecewise lines is that it provides us a way to treat concave decision regions. The piecewise lines

used in this research were selected manually based on the actual measurement data. This method is not further discussed in the dissertation.

7.3.5 Classification results

As stated above, by inserting the explosive simulants into common bags, we can investigate object classification under various scenarios. More than one hundred scenarios were created and scanned to verify the performance of the prototype x-ray scanning system. Some typical image examples scanned by using the prototype scanning system have been shown in Section 7.2.2. The dual-energy and scatter-energy values for some materials are given in the following tables.

Table 7.3-1 shows observed transmission and scatter values as well as the computed (R, L) values for six explosive simulants (images given in Figure 7.2-4). The transmissions and scatters as well as the computed (R, L) values for three step wedges are shown in Tables 7.3-2 to 7.3-4 (see Figures 7.2-6 to 7.2-8 for scatter images, and Figures 5.1-7 to 5.1-9 for transmission images).

With (R, L) values given in Tables 7.3-1 to 7.3-4, we will show an example to derive the decision rules based on our discussion in Section 7.3.4.

Let's consider the 2-class case as follows, "explosive materials" (C_2: data given in Table 7.3-1) and "other organic materials" (C_1: data given in Tables 7.3-3 and 7.3-4). "Inorganic materials", such as aluminum, are not included in our discussion because it can be easily eliminated by pre-using a piece-wise line boundary due to their big distance to "explosive materials".

Table 7.3-1 R and L values for six explosive simulants.

Simulants	T_L	T_H	B_L	F_L	R	L
Smokeless powder	65.7	93.7	168.0	127.1	1.0332	1.2784
Ammonia nitrate (high density)	34.3	71.5	136.0	68.2	1.2647	1.3950
Black powder	24.8	65.4	92.2	34.8	1.4772	1.3569
Semtex	55.5	85.9	172.9	116.8	1.0847	1.3346
Dynamite	35.7	69.9	151.1	91.5	1.2188	1.4391
Ammonia nitrate (low density)	36.1	65.3	162.4	94.5	1.0836	1.4492

Table 7.3-2 R and L values for aluminum step wedge.

Thickness (cm)	T_L	T_H	B_L	F_L	R	L
0.259	139.3	179.5	85.2	57.9	2.9188	0.8680
0.508	112.9	167.1	83.7	65.9	2.9356	0.9280
0.711	98.1	158.1	83.3	67.4	2.8762	0.9611
1.014	81.2	146.0	82.1	69.8	2.9487	1.0078
1.189	73.2	139.2	78.0	72.2	2.8235	1.0325
1.392	66.1	131.8	75.9	74.3	2.9302	1.0561
1.524	62.0	127.5	73.5	74.1	2.9543	1.0709
2.032	48.4	111.7	62.9	65.6	2.8164	1.1260

Table 7.3-3 R and L values for clear plastic step wedge.

Thickness (cm)	T_L	T_H	B_L	F_L	R	L
0.635	176.6	178.2	81.3	78.7	1.3554	0.8675
1.27	158.4	168.6	109.6	106.7	1.2736	0.9604
1.905	145.0	160.2	128.5	124.2	1.2747	1.0149
2.54	132.1	151.3	142.0	134.5	1.2392	1.0560
3.18	121.4	143.6	152.3	140.0	1.2251	1.0885
3.81	111.4	136.2	159.0	143.6	1.3052	1.1173
4.45	102.4	128.5	165.7	145.3	1.2521	1.1449
5.08	94.5	122.1	171.0	146.3	1.2275	1.1706
5.72	86.7	114.8	174.3	147.5	1.2875	1.1975
6.35	80.7	109.8	177.7	148.6	1.2651	1.2210

Table 7.3-4 R and L values for white plastic step wedge.

Thickness (cm)	T_L	T_H	B_L	F_L	R	L
0.635	181.4	177.8	69.5	77.3	1.0768	0.8459
1.27	164.6	168.6	93.8	107.9	1.1154	0.9393
1.905	150.7	159.7	110.6	127.4	1.0610	0.9951
2.54	138.7	151.1	122.9	140.0	1.0657	1.0355
3.18	127.7	142.6	132.8	147.8	1.0364	1.0690
3.81	117.8	135.3	141.5	153.2	1.0684	1.0992
4.45	109.0	128.2	147.2	156.2	1.0762	1.1250
5.08	100.8	121.2	152.6	158.9	1.0794	1.1509
5.72	92.9	114.4	157.1	160.0	1.1297	1.1765
6.35	86.2	108.3	160.4	160.7	1.1399	1.2001
6.99	80.0	102.7	163.7	161.6	1.0711	1.2246
7.62	74.2	97.1	165.8	162.1	1.0951	1.2484
8.26	68.9	91.7	168.2	162.9	1.0475	1.2743
8.89	63.9	86.9	169.4	163.7	1.1032	1.2987
9.53	59.1	82.2	170.3	164.5	1.0764	1.3255

(1) Normal density functions

For a two-dimensional variable $x = [x_1 \quad x_2]^T$, its mean value μ, covariance matrix Ω, and normal density function $p(x)$ can be written as follows:

$$\mu = [\mu_1 \quad \mu_2]^T \tag{7.11}$$

where $\mu_i = \frac{1}{N}\sum_{j=1}^{N} x_{ij}$, and N is the number of samples;

$$\Omega = \begin{bmatrix} \omega_{11} & \omega_{12} \\ \omega_{21} & \omega_{22} \end{bmatrix} \tag{7.12}$$

where $\omega_{kl} = \frac{1}{N-1}\sum_{j=1}^{N}(x_{kj} - \mu_k)(x_{lj} - \mu_l)$;

$$p(x) = \frac{1}{2\pi|\Omega|^{1/2}} \exp\left\{-\frac{1}{2}(x-\mu)^{\mathrm{T}}\ \Omega^{-1}\ (x-\mu)\right\} \tag{7.13}$$

(2) Discriminant function

The discriminant function for class i can be obtained by taking logarithm on (7.13) and by removing the constant away from the equation, yielding,

$$g_i(x) = x^T W_i x + w_i^T x + w_{0i} \tag{7.14}$$

where $W_i = -\Omega^{-1}$, $w_i = 2\,\Omega_i^{-1}\mu_i$, and $w_{0i} = -\mu_i^T \Omega_i^{-1}\mu_i - \log(|\Omega_i|)$.

(3) Decision boundary

For class C_1: "other organic materials", its mean value μ_1 and covariance matrix Ω_1 can be obtained directly by using (7.11) and (7.12):

$$\mu_1 = \begin{bmatrix} \mu_{1R} \\ \mu_{1L} \end{bmatrix} = \begin{bmatrix} 1.1579 \\ 1.1139 \end{bmatrix} \tag{7.15}$$

$$\Omega_1 = \begin{bmatrix} 0.0099 & -0.0029 \\ -0.0029 & 0.0164 \end{bmatrix} \tag{7.16}$$

For class C_2: "explosive materials", we have,

$$\mu_2 = \begin{bmatrix} \mu_{2R} \\ \mu_{2L} \end{bmatrix} = \begin{bmatrix} 1.1937 \\ 1.3755 \end{bmatrix} \tag{7.17}$$

$$\Omega_2 = \begin{bmatrix} 0.0272 & 0.0019 \\ 0.0019 & 0.0043 \end{bmatrix} \tag{7.18}$$

By submitting Equations (7.15) and (7.16) into (7.14), we obtain the discriminant function $g_1(R, L)$ for class 1,

$$g_1(R,L) = -106.86R^2 - 64.43L^2 - 38.20RL + 290.00R + 187.76L - 263.68 \qquad (7.19)$$

Similarly we have $g_2(R,L)$ for class 2,

$$g_2(R,L) = -38.04R^2 - 242.48L^2 + 34.41RL + 43.48R + 626.00L - 447.40 \qquad (7.20)$$

The decision boundary is therefore obtained with $g_2(R,L) - g_1(R,L) = 0$, yielding,

$$D(R,L) = 68.82R^2 - 178.05L^2 + 72.61RL - 246.52R + 438.24L - 183.71 = 0 \qquad (7.21)$$

(4) Decision rules

Equations (7.19) and (7.20) represent two ellipses in 2-dimensional space. The tie between them results in a hyperbola (7.21). The decision rules therefore can be stated as follows: for any object having a (R, L) value, if its $D(R,L)$ is greater than zero, we decide it as "explosive materials" (shown as dark area in Figure 7.3-4); otherwise it is decided to be "other organic materials".

We started our test with simple luggage bags, then with overlapping materials having regular shapes, finally with overlapping materials having irregular shapes. The probability of correct classification was improved to 82% based on lab verifications from system group. By correct classification it means that no explosives missed detection, and no other types of materials were identified as threat.

It should be noted that to achieve a good performance, every part in the prototype system should work properly. During our experimental study on object classification for real luggage, it was found that the major problem lies with overlapping objects, where the true

signal intensity of transmission and scatter images should be uniquely provided for each object. More analysis on this issue is available in [LU99]. Also, we found that there is some overlap between innocent articles and the compositions of explosive simulants, for example, between white plastic and smokeless powder. Therefore, we are not surprised that plastic is used as an explosive simulant adopted by FAA.

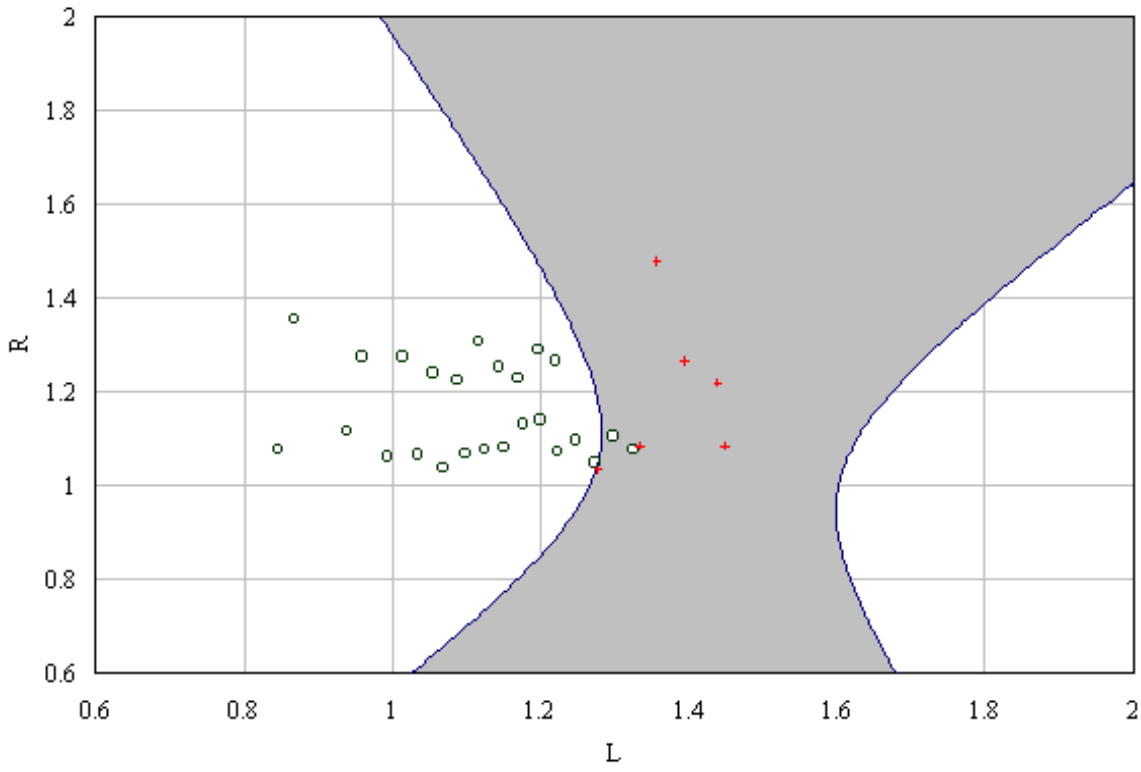

Figure 7.3-2 An example on decision boundary for discriminating two-class materials.